


ARTICLE



Expression of actin- and oxidative phosphorylation-related transcripts across the cortical visuospatial working memory network in unaffected comparison and schizophrenia subjects

Sohei Kimoto^{1,7,8}, Takanori Hashimoto^{2,3,4,8}, Kimberly J. Berry³, Makoto Tsubomoto², Yasunari Yamaguchi^{1,7}, John F. Enwright³, Kehui Chen^{3,5}, Rika Kawabata², Mitsuru Kikuchi^{2,4}, Toshifumi Kishimoto¹ and David A. Lewis^{3,5,6} 

© The Author(s), under exclusive licence to American College of Neuropsychopharmacology 2022

Visuospatial working memory (vsWM), which is impaired in schizophrenia (SZ), is mediated by a distributed cortical network. In one node of this network, the dorsolateral prefrontal cortex (DLPFC), altered expression of transcripts for actin assembly and mitochondrial oxidative phosphorylation (OXPHOS) have been reported in SZ. To understand the relationship between these processes, and the extent to which similar alterations are present in other regions of vsWM network in SZ, a subset of actin- (CDC42, BAIAP2, ARPC3, and ARPC4) and OXPHOS-related (ATP5H, COX4I1, COX7B, and NDUF3) transcripts were quantified in DLPFC by RNA sequencing in 139 SZ and unaffected comparison (UC) subjects, and in DLPFC and three other regions of the cortical vsWM network by qPCR in 20 pairs of SZ and UC subjects. By RNA sequencing, levels of actin- and OXPHOS-related transcripts were significantly altered in SZ, and robustly correlated in both UC and SZ subject groups. By qPCR, cross-regional expression patterns of these transcripts in UC subjects were consistent with greater actin assembly in DLPFC and higher OXPHOS activity in primary visual cortex (V1). In SZ, CDC42 and ARPC4 levels were lower in all regions, BAIAP2 levels higher only in V1, and ARPC3 levels unaltered across regions. All OXPHOS-related transcript levels were lower in SZ, with the disease effect decreasing from posterior to anterior regions. The differential alterations in markers of actin assembly and energy production across regions of the cortical vsWM network in SZ suggest that each region may make specific contributions to vsWM impairments in the illness.

Neuropsychopharmacology (2022) 47:2061–2070; <https://doi.org/10.1038/s41386-022-01274-9>

INTRODUCTION

Certain core cognitive impairments, such as working memory (WM) deficits [1], have a major influence on the long-term functional outcomes of individuals with schizophrenia (SZ) [2]. Visuospatial WM (vsWM) is predominantly mediated by coordinated neural activity across a distributed cortical neural network that includes nodes in primary (V1) and association (V2) visual regions of the occipital lobes which convey visual information to nodes in the posterior parietal cortex (PPC) and dorsolateral prefrontal cortex (DLPFC) [3, 4]. The activity of excitatory pyramidal neurons that provide the connections among these cortical nodes is shaped by the activity of local inhibitory neurons that are, in turn, influenced by excitatory inputs from neighboring pyramidal neurons [5–7].

In individuals with SZ, multiple postmortem studies have revealed structural and molecular alterations in cellular components that regulate the excitatory synaptic transmission required for WM performance [8, 9]. For example, a lower density of dendritic spines, the sites of most excitatory synaptic inputs to pyramidal neurons [10–12], and altered expression of transcripts

for the regulators of actin cytoskeleton, which play a critical role in the formation and maintenance of dendritic spines [13–16], have been reported in the DLPFC of subjects with SZ.

In addition, ATP synthesis via mitochondrial oxidative phosphorylation (OXPHOS), which supports energetic demand of the neuronal activity and synaptic transmission required for WM performance [17–19], appears to be impaired in the DLPFC of subjects with SZ [20–24]. Consistent with these findings, lower levels of OXPHOS-related transcripts have been reported in DLPFC pyramidal neurons from subjects with SZ [25, 26].

Expression of actin- and OXPHOS-related transcripts would be expected to be correlated as dendritic spine density influences pyramidal neuron activity and hence the demand for energy production [17, 27], and at the same time, energy production is crucial for the maintenance of dendritic spines [28, 29]. Furthermore, since both the number of dendritic spines on layer 3 pyramidal neurons [30–33] and mitochondrial energy production [34, 35] have been reported to differ across cortical regions, levels of actin- and OXPHOS-related transcripts are expected to differ across regions of the vsWM network in UC subjects. Finally, in SZ

¹Department of Psychiatry, Nara Medical University School of Medicine, Kashihara 634-8521, Japan. ²Department of Psychiatry and Behavioral Science, Kanazawa University Graduate School of Medical Sciences, Kanazawa 920-8640, Japan. ³Department of Psychiatry, University of Pittsburgh, Pittsburgh, PA 15213, USA. ⁴Research Center for Child Development, Kanazawa University, Kanazawa 920-8640, Japan. ⁵Department of Statistics, University of Pittsburgh, Pittsburgh, PA 15213, USA. ⁶Department of Neuroscience, University of Pittsburgh, Pittsburgh, PA 15213, USA. ⁷Present address: Department of Neuropsychiatry, Wakayama Medical University School of Medicine, Wakayama 641-8509, Japan. ⁸These authors contributed equally: Sohei Kimoto, Takanori Hashimoto. ✉email: lewisda@upmc.edu

Received: 25 August 2021 Revised: 5 January 2022 Accepted: 6 January 2022

Published online: 15 January 2022

subjects, lower spine density is more prominent in the DLPFC compared to V1 [10], suggesting that actin-related transcripts should exhibit regionally different alterations within the vsWM network in SZ subjects. Therefore, comparing the cross-regional alterations between actin- and OXPHOS-related transcripts in SZ subjects might provide an insight into relationship between lower dendritic spine density and less energy production across the regions of the vsWM network in SZ.

In the present study, using the RNA sequencing (RNAseq) data generated by the CommonMind Consortium in DLPFC total gray matter samples from 82 UC and 57 SZ subjects [36], we first examined transcript levels and cross correlations of a subset of key actin- and OXPHOS-related molecules. Next, we employed quantitative PCR (qPCR) to determine the levels of these same transcripts in total gray matter samples from the DLPFC and three other cortical regions (primary (V1) and secondary (V2) visual cortices, and PPC) of the vsWM network from 20 matched pairs of UC and SZ subjects. Then, we compared the effect of SZ on the expression of actin- and OXPHOS-related transcripts across these regions.

METHODS

Human subjects

Brain specimens were obtained during routine autopsies conducted at the Allegheny County Medical Examiner's Office (Pittsburgh, PA) following consent from the next-of-kin. An independent committee of experienced research clinicians made consensus DSM-IV diagnoses for each subject or confirmed the absence of any psychiatric or neurological diagnoses, based on the results of structured interviews conducted with family members and review of medical records, neuropathology exam and toxicology testing. All procedures were approved by the University of Pittsburgh's Committee for the Oversight of Research and Clinical Training Involving Decedents and Institutional Review Board for Biomedical Research, as well as by the Ethics committees of Nara Medical University and Kanazawa University Graduate School of Medical Sciences.

Selection of transcripts used in the current study

We selected 4 actin- (BAIAP2, CDC42, ARPC3, and ARPC4) and 4 OXPHOS-related (NDUFB3, COX411, COX7B and ATP5H) transcripts. Expression levels of these 8 transcripts were all previously reported to be altered in the DLPFC from SZ subjects in studies using different quantification methods at different anatomical resolutions [13–16, 25, 26, 37, 38]. Among the actin-related transcripts, the Rho GTPase CDC42, a central regulator of actin assembly that is essential for neuronal morphology, promotes spine growth and stability [39], whereas BAIAP2 inhibits actin assembly and thus suppresses spine growth [40, 41]. ARPC3 and ARPC4 link CDC42-dependent signals to actin assembly and are required for dendritic spine formation and maintenance [42]. For OXPHOS-related transcripts, each

transcript encodes a component of key complexes for mitochondrial electron transfer chain [43, 44]: NDUFB3 for NADH dehydrogenase (complex I), COX411 and COX7B for cytochrome oxidase (complex IV), and ATP5H for ATP synthase (complex V). The expression levels of these OXPHOS-related transcripts are normally coordinated in response to changes in the energetic demand in neurons [27, 45].

These actin- and OXPHOS-related transcripts have multiple isoforms derived from alternative splicing. Our qPCR primer sets for ARPC3, ARPC4, NDUFB3, COX7B, and ATP5H amplified a fragment that is common to all reported isoforms. For BAIAP2, CDC42 and COX411, our qPCR primer sets amplified a fragment that is selective to some isoforms. These fragments are adjacent or within the sequences recognized by the microarray probes that detected altered expression levels of these transcripts in our previous study [25].

RNA sequencing (RNAseq) subject cohort and analysis

RNAseq data used in these analyses included a subset of the data generated by the CommonMind Consortium (https://www.nimhgenetics.org/available_data/commonmind/). Principal component analysis of the DLPFC samples revealed institution as a major source of variance. Therefore, to eliminate this unwanted source of variance, only University of Pittsburgh subjects ($n = 139$) were used in the transcriptome analysis of the current study (Table 1, Supplementary Table 1a). Subject groups did not differ in mean age, pH, RNA integrity number (RIN) (Agilent Bioanalyzer, Agilent Technologies, CA), postmortem interval (PMI), or tissue storage time at -80°C (Table 1). Total RNA was isolated from gray matter tissues of right DLPFC (area 9/46) of each subject and subjected to RNAseq as described previously [36] and in Supplementary Methods.

Quantitative PCR (qPCR) subject cohort and analysis

To control for experimental variance and to reduce biological variance between the groups of UC ($n = 20$) and SZ ($n = 20$) subjects, each SZ subject was individually matched to one UC subject for sex and as closely as possible for age (Table 1, Supplementary Table 1b). The two groups did not differ in mean age, pH, RIN, PMI, or tissue storage time (Table 1). Total RNA was isolated from gray matter samples of all four cortical regions (V1, V2, PPC, and DLPFC) of the right hemisphere of each subject (Supplementary Fig. 1) and used for qPCR amplification of transcripts of interest and two internal reference transcripts (β -actin and glyceraldehyde-3-phosphate dehydrogenase) with specific primer sets (Supplementary Table 3). Samples from members of a subject pair were always processed together throughout all stages of an experiment. Transcript levels were determined based on the difference between the cycle threshold (CT) of the target transcript and the mean CT of internal reference transcripts. See Supplementary Methods for details.

Statistical analyses

For RNAseq data analysis, genes with 0 counts in at least 50% of the samples were removed and the remaining 14,428 genes were subjected to normalization and confidence weight calculation using the LIMMA

Table 1. Summary of cohort characteristics and methods for mRNA quantification.

Characteristic	RNA seq				Quantitative PCR			
	Unaffected Comparison		Schizophrenia		Unaffected Comparison		Schizophrenia	
	(n = 82)		(n = 57)		(n = 20)		(n = 20)	
	Male	Female	Male	Female	Male	Female	Male	Female
Sex	59	23	44	13	14	6	14	6
	White	Black	White	Black	White	Black	White	Black
Race	71	11	41	16	15	5	14	6
	Mean	SD	Mean	SD	Mean	SD	Mean	SD
Age (years)	48.2	14.2	48.1	13.0	45.4	11.6	44.3	10.4
Postmortem interval (hours)	19.0	5.4	20.0	8.4	15.4	5.8	14.3	6.4
Brain pH	6.7	0.3	6.6	0.3	6.7	0.3	6.5	0.3
RNA integrity number	8.5	0.4	8.2	0.6	8.3	0.4	8.3	0.6
Storage time (months at -80°C)	106.7	56.6	111.5	60.5	111.9	41.3	113.0	48.8

A

	Transcript	Ensembl Gene ID	q value	% difference
Actin assembly	BAIAP2	ENSG00000175866	0.005	26.4
	CDC42	ENSG00000070831	<0.001	-17.1
	ARPC3	ENSG00000111229	0.012	-12.3
	ARPC4	ENSG00000241553	0.015	-12.9
OXPHOS*	NDUFB3	ENSG00000119013	<0.001	-22.3
	COX4i1	ENSG00000131143	0.004	-15.4
	COX7B	ENSG00000131174	<0.001	-18.5
	ATP5H	ENSG00000167863	0.006	-16.3

*OXPHOS, oxidative phosphorylation

B

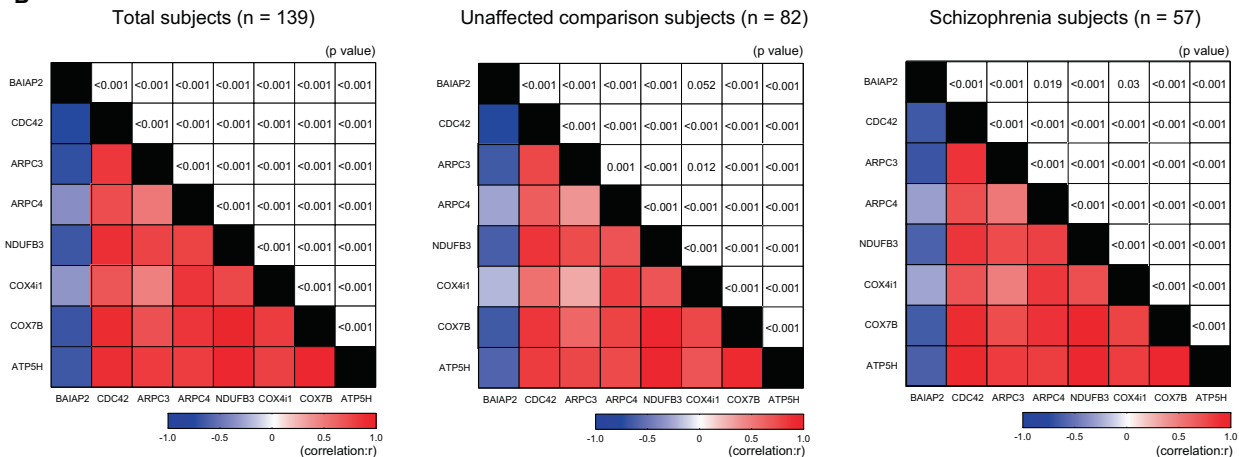


Fig. 1 Differential expression and cross-correlation analysis of actin- and OXPHOS-related transcripts assessed by RNAseq in DLPFC gray matter of unaffected comparison and schizophrenia subjects. **A** RNAseq data of mean differences between SZ and UC subjects in actin- and OXPHOS-related transcripts in the DLPFC. **B** Matrix of cross-correlations among the transcripts in total (left), unaffected comparison (middle) and schizophrenia (right) subject groups. Correlation coefficients for each combination of two transcripts are shown in the lower left part of the matrix according to the color bar at the bottom, and corresponding p values are shown in the upper right part.

package [46] in R. The normalized read counts and confidence weights were used to determine differential gene expression using a basic linear regression model with age, sex, RIN, PMI, and five ancestry-related factors included as covariates. Statistical significance was determined using the Benjamini-Hochberg procedure on the resulting p values with a false discovery rate of 5%. Levels of actin- and OXPHOS-related molecules identified in the differential-expression analysis were subjected to Pearson correlation analysis.

For the cross-regional analysis by qPCR, we used mixed models treating observations from the four regions of each subject as repeated measurements to account for the within-subject correlation among four regions and to characterize the within- and between-subject variability (see Supplementary Methods for details). To assess differences in the target transcript levels across the four regions in UC subjects, the model included transcript as the dependent variable, region as a fixed effect, and age, sex, brain pH, RIN, PMI and RNA ratio as covariates. F-tests were used to assess the overall regional effect, followed by post hoc pairwise comparisons between regions. To determine if the expression of these transcripts was altered in SZ, the mixed model included transcript level as the dependent variable, diagnosis, region, and diagnosis-by-region interaction as the fixed effects, and the same set of covariates. If the diagnosis-by-region interaction was significant, we also assessed the diagnosis effect in each region. Benjamini-Hochberg adjusted p values were computed to control for multiple comparison across eight transcripts [47], and reported p values for each transcript have been adjusted to correspond to the false discovery rate of 5%. In each of V1, V2, PPC and DLPFC, cross correlations among actin- and OXPHOS-related transcripts were assessed by Pearson correlation analyses. All analyses of individual transcripts were conducted on log-transformed data. The potential confounding effect of antipsychotic medications, nicotine, or other substances of abuse, suicide, and other factors frequently comorbid with SZ was also examined by using Student *t* test (Supplementary Table 4).

Composite measures for actin assembly and OXPHOS were computed by the sum of the normalized (Z-score) expression levels for each of the

actin- and OXPHOS-related transcripts, respectively (see Supplementary Methods). Since BAIAP2 has an inhibitory regulation, as opposed to the promoting effects of CDC42, ARPC3 and ARPC4, on actin assembly, we added minus signs to its Z-scores before summing Z-scores for all transcripts. For each composite measure, the mixed model was performed as described above. In order to address the risk of false positive findings, we conducted a Bayesian repeated measures analysis of variance (ANOVA) on the composite measures using JASP (<https://jasp-stats.org>) [48]. This analysis included the composite measures from the four regions of each subject as repeated measures, diagnosis as the between-subject factor and the same set of covariates as in the mixed model.

RESULTS

Transcript levels for actin- and OXPHOS-related pathways in DLPFC of UC and SZ subjects by RNAseq

Our analysis of RNAseq data found altered expression levels of the 4 actin- and 4 OXPHOS-related transcripts (all $q < 0.05$) (Fig. 1A). Among actin-related transcripts, BAIAP2 mRNA levels were higher by 26%, whereas levels of other three transcripts were lower by -12% to -17% in SZ subjects. All OXPHOS transcripts exhibited lower levels by -15 to -22% in SZ subjects. These results are consistent with prior reports [13–16, 25, 26, 37, 38], including our use of a different analytical strategy to assess OXPHOS-related transcripts in the same UC and SZ subjects [26]. Importantly, levels of all actin- and OXPHOS-related transcripts were significantly correlated (all $r > |0.21|$) with each other in the UC, SZ and combined groups of subjects (Fig. 1B), consistent with the idea that dendritic spine density and energy production are related in the DLPFC. All transcripts were positively correlated with each other except for BAIAP2 which, as expected based on its inhibitory

role in actin assembly, was negatively correlated with the other actin- and all OXPPOS-related transcripts.

Expression of actin- and OXPPOS-related transcripts in the vsWM network in UC subjects

Among actin-related transcripts, BAIAP2 mRNA levels were highest in V1 and V2 and progressively declined from posterior to anterior regions, with intermediate levels in PPC and lowest levels in the DLPFC ($F_{3,57} = 49.6, p < 0.001$) (Fig. 2A). In contrast, CDC42 mRNA levels ($F_{3,57} = 17.0, p < 0.001$) were highest in DLPFC, intermediate in V1 and lowest in V2 and PPC (Fig. 2B). Levels of both ARPC3 ($F_{3,57} = 3.33, p = 0.026$) and ARPC4 ($F_{3,57} = 11.2, p < 0.001$) mRNAs were highest in DLPFC and did not differ across the other three regions (Fig. 2C, D).

All four OXPPOS-related transcripts showed declined from posterior to anterior regions. Levels of NDUFB3 ($F_{3,57} = 15.3, p < 0.001$), COX411 ($F_{3,57} = 34.3, p < 0.001$) and ATP5H ($F_{3,57} = 24.3, p < 0.001$) mRNAs were highest in V1, intermediate in V2, and lowest in PPC and DLPFC (Fig. 2E, F, H). Similarly, COX7B mRNA levels ($F_{3,57} = 24.9, p < 0.001$) were highest in V1, intermediate in V2 and PPC, and lowest in DLPFC (Fig. 2G).

Effect of SZ on actin- and OXPPOS-related transcript levels in the vsWM network

For BAIAP2 mRNA, our mixed model detected significant effects of region ($F_{3,114} = 83.2, p < 0.001$) and a diagnosis-by-region interaction ($F_{3,114} = 4.93, p = 0.006$) without a significant diagnosis effect ($F_{1,32} = 1.46, p = 0.27$) (Fig. 3A). Post hoc analysis revealed that BAIAP2 mRNA levels were unaltered in V2, PPC and DLPFC, but were significantly upregulated in V1 ($p = 0.007$) of SZ subjects. Levels of CDC42 and ARPC4 mRNAs significantly differed by diagnosis ($F_{1,32} = 10.27, p = 0.005$ and $F_{1,32} = 5.78, p = 0.029$, respectively) and by region ($F_{3,114} = 16.1, p < 0.001$ and $F_{3,114} = 23.1, p < 0.001$, respectively), but the interaction term was not significant (Fig. 3B, D). CDC42 and ARPC4 mRNA levels were lower in all four cortical regions of the vsWM network in SZ subjects. Finally, ARPC3 mRNA expression showed neither an effect of diagnosis nor a diagnosis-by-region interaction, but the effect of region on mRNA level was significant ($F_{3,114} = 5.41, p = 0.002$) (Fig. 3C).

All OXPPOS-related transcripts (Fig. 3E–H) exhibited significant effects of diagnosis (all $F_{1,32} > 10.2$, all $p < 0.006$) and region (all $F_{3,114} > 3.2$, all $p < 0.03$), as well as a diagnosis-by-region interaction (all $F_{3,114} > 4.7$, all $p < 0.006$). Post hoc analyses showed that NDUFB3 and ATP5H mRNA levels (Fig. 3E, H) were significantly lower in V1 and V2 (both $p < 0.001$), but were unaltered in PPC and DLPFC (all $p > 0.07$), of SZ subjects. COX411 mRNA levels (Fig. 3F) were significantly lower in V1, V2 and DLPFC (all $p < 0.05$), respectively, but were unaltered in PPC ($p = 0.08$), and COX7B mRNA levels (Fig. 3G) were significantly lower in V1, V2 and PPC (all $p < 0.03$), but were unaltered in DLPFC of SZ subjects.

We tested cross correlations between actin- and OXPPOS-related transcripts in V1, V2, PPC and DLPFC using qPCR data. In contrast to the robust correlations detected in DLPFC RNAseq data of 82 comparison and 57 schizophrenia subjects, correlations among transcript levels were much less prominent in each region, presumably due to the limited sample size (20 pairs of UC and SZ subjects). However, we detected that cross-correlations between actin- and OXPPOS-related transcripts were weaker in A17 and A18 than in A46 and A7 (Supplementary Fig. 2).

Composite measures of actin- and OXPPOS-related transcripts across the vsWM network

To obtain aggregate indices of actin assembly and mitochondrial energy production across regions of the visuospatial WM network, we computed composite actin and OXPPOS measures from the normalized expression levels of the four transcripts in each category (Fig. 4). In UC subjects, the composite actin ($F_{3,114} = 25.8$,

$p < 0.001$) and OXPPOS ($F_{3,114} = 20.1, p < 0.001$) measures significantly differed across regions (Fig. 4A, B). The composite actin measure was greatest in DLPFC and did not differ across the other three regions, whereas the composite OXPPOS measure was greatest in V1 and progressively decreased from posterior to anterior regions of the vsWM network (Fig. 4A, B).

Relative to UC subjects, the composite actin measure (Fig. 4A) was lower in all regions of SZ subjects, exhibiting significant differences by diagnosis ($F_{1,32} = 5.95, p = 0.02$) and region ($F_{3,114} = 40.9, p < 0.001$), without a significant interaction between diagnosis and region ($F_{3,114} = 0.8, p = 0.50$). For the composite OXPPOS measure (Fig. 4B), the posterior-to-anterior gradient was absent in the SZ subjects, as indicated by significant effects of diagnosis ($F_{1,32} = 17.4, p < 0.001$), region ($F_{3,114} = 12.1, p < 0.001$) and diagnosis-by-region interaction ($F_{3,114} = 8.25, p < 0.001$).

Bayesian repeated measures ANOVA [48] on the composite measures supported strongly the likelihood of the models including the factors with the significant effects in the mixed models, rejecting the alternative models without these factors. For the composite actin measures, the Bayesian Factors computed for diagnosis and regions were 4.6 and 5.4×10^{15} , respectively, providing substantial and decisive evidence of the effects of these factors [49]. For the composite OXPPOS measures, the Bayesian Factors for diagnosis, region, and diagnosis-by-region interaction were 702, 4124 and 443, respectively, decisively supporting the effects of these factors.

DISCUSSION

Normal vsWM processes require information transfer across multiple nodes in the neocortex, including visual, posterior parietal, and dorsolateral prefrontal regions. Previous studies reported altered levels of transcripts involved in the regulation of actin assembly and ATP synthesis via OHPHOS in the DLPFC of subjects with SZ [13–16, 20, 25, 37], but the relationships among these transcripts and whether these transcript levels differ across regions in the vsWM network of UC and SZ subjects were unknown.

Actin- and OXPPOS-related transcripts in the DLPFC of UC and SZ subjects

A subset of representative molecules in the actin signaling (BAIAP2, CDC42, ARPC3 and ARPC4) and OXPPOS pathways (NDUFB3, COX411, COX7B and ATP5H) were reported to be differently expressed in the DLPFC from subjects with SZ using different levels of anatomical resolution and different quantification methods [13–16, 25, 37]. Thus, we investigated the expression levels of these 8 transcripts in the RNAseq data from DLPFC total gray matter in a larger cohort of 57 subjects with schizophrenia and 82 unaffected comparison subjects. In our RNAseq data, we verified altered expression levels of all actin-related transcripts in the DLPFC of SZ subjects (Fig. 1), providing both biological and technical replication of the prior findings. Given that BAIAP2 is a negative regulator of actin assembly, the reciprocal alterations between BAIAP2 and the other actin-related transcripts (CDC42, ARPC3 and ARPC4) in the DLPFC of SZ subjects might represent a molecular mechanism for deficient actin assembly that could contribute to the morphological alterations in DLPFC pyramidal cells, such as smaller cell bodies, shorter dendritic length and lower density of dendritic spines reported in SZ [10–12, 50]. We recently reported that many transcripts in the OXPPOS pathway were down-regulated in a coordinated manner in the DLPFC of SZ subjects [26], and the present reanalysis of these data using a different statistical model confirmed a conserved effect of SZ on the four OXPPOS-related transcripts examined here. Furthermore, the correlated expression among actin- and OXPPOS-related transcripts in both subject groups is consistent with the idea that disturbed actin assembly in dendritic spines might result in

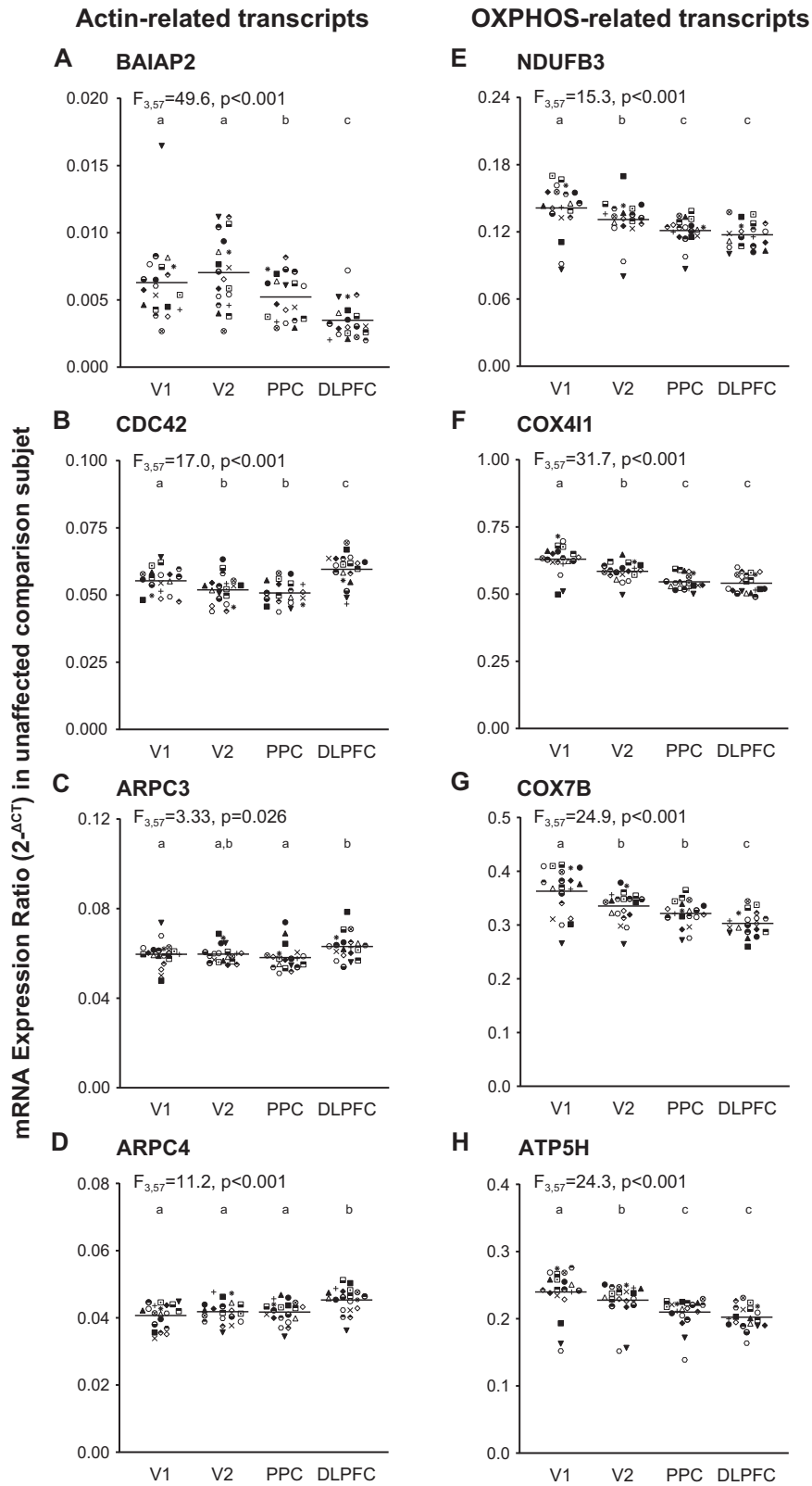


Fig. 2 Expression levels of actin- and OXPHOS-related transcripts across the four cortical regions of the visuospatial WM network in unaffected comparison subjects. For each (A–H), transcript name and the mixed model results are shown at the top left. Transcript levels of individual subjects are shown by the same symbol in all graphs. Horizontal bars represent group means. For each transcript, regions within each graph that do not share the same letter are significantly different by post hoc comparisons ($p < 0.05$). V1 primary visual cortex, V2 association visual cortex, PPC posterior parietal cortex, DLPFC dorsolateral prefrontal cortex.

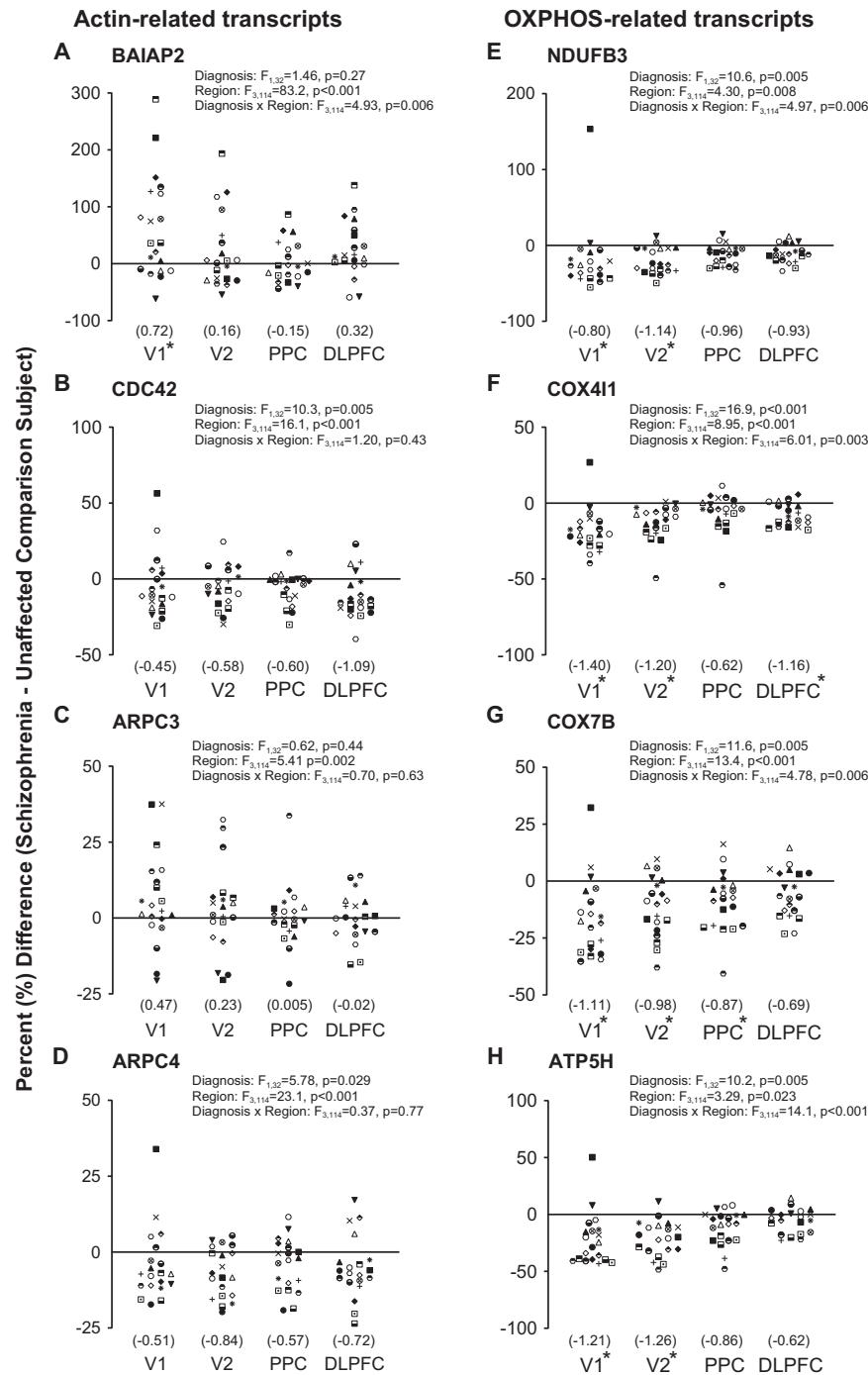


Fig. 3 Effect of schizophrenia on actin- and OXPPOS-related transcripts across the four cortical regions of the visuospatial WM network. For each (A–H), transcript name is at the top left and the mixed model result at the top center. Across regions, % difference of transcript levels between unaffected comparison (UC) and schizophrenia (SZ) subjects in each subject pair are shown by the symbols from Fig. 2 that corresponds to the unaffected comparison subject in that pair. Horizontal bars represent mean percent difference across subject pairs. Values in parentheses represent Cohen's D effect size in each region for each transcript between SZ and UC subjects. An asterisk (*) indicates significant difference between the UC and schizophrenia subjects ($p < 0.05$) in each region on post hoc comparisons that were performed when the mixed model detected a significant diagnosis-by-region interaction. V1 primary visual cortex, V2 association visual cortex, PPC posterior parietal cortex, DLPFC dorsolateral prefrontal cortex.

reduced pyramidal cell activity and a lower requirement for mitochondrial energy production [25, 26, 29, 51].

As genome wide-association studies have implicated genes involved in the regulation of dendritic spines and mitochondrial functions in the pathogenesis of SZ [52, 53], we evaluated the association between polygenic risk scores (PRS) that were

determined based on the data of PGC and CLOZUK cohort [54] and our DLPFC RNAseq data from 139 subjects. We did not find any significant correlations between PRS determined with three different statistical thresholds and DLPFC levels of any of the transcripts of interest in either control (all $r < |0.19|$) or schizophrenia (all $r < |0.22|$) subject groups.

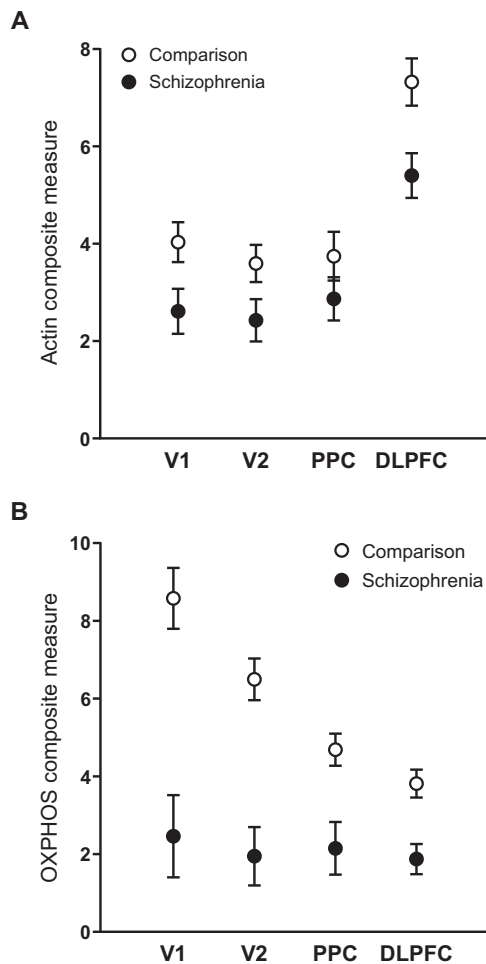


Fig. 4 Effect of schizophrenia on composite measures of actin- and OXPPOS-related transcripts in the visuospatial WM network. In unaffected comparison (UC) subjects, the composite (A) actin ($F_{3,114} = 25.8$, $p < 0.001$) and (B) OXPPOS ($F_{3,114} = 20.1$, $p < 0.001$) significantly differed across regions. In comparisons between UC and SZ subjects, the actin composite measure significantly differed by diagnosis ($F_{1,32} = 5.95$, $p = 0.02$) and region ($F_{3,114} = 40.9$, $p < 0.001$), but the interaction term was not significant ($F_{3,114} = 0.8$, $p = 0.50$). For the OXPPOS composite measure, the caudal-to-rostral gradient was absent in the SZ subjects, as indicated by significant effects of diagnosis ($F_{1,32} = 17.4$, $p < 0.001$), region ($F_{1,32} = 12.1$, $p < 0.001$) and diagnosis-by-region interaction ($F_{3,114} = 8.25$, $p < 0.001$). Error bars indicate the standard error of the mean (SEM). V1 primary visual cortex, V2 association visual cortex, PPC posterior parietal cortex, DLPFC dorsolateral prefrontal cortex.

Expression of transcripts across regions of the cortical WM network in UC subjects

Both actin- and OXPPOS-related transcripts exhibited distinctive cross-regional expression patterns in vsWM network of UC subjects. Transcript levels of CDC42, ARPC3 and ARPC4, positive regulators of actin assembly [42], were highest in DLPFC and lowest in V1, whereas levels of BAIAP2, which negatively regulates actin assembly and spine formation [40, 41], were highest in occipital cortex (V1 and V2) and declined from posterior to anterior regions. Together, these findings suggest that across the vsWM cortical network the molecule substrate for actin regulation is greatest in DLPFC and lowest in V1. Interestingly, in nonhuman primates the dendritic field areas of pyramidal neurons were 1.3 times, 2.5–3.5 times, and >5 times larger in V2, PPC, and DLPFC, respectively, than in V1 [32, 33]. The total number of dendritic branches per pyramidal neuron, as well as the number and density

of spines, showed a similar posterior-to-anterior increase [30–33]. Therefore, relative to the other cortical regions, the lower expression of BAIAP2 and the higher expression of CDC42, ARPC3 and ARPC4 (Fig. 2A–D) in the DLPFC could contribute to the greater spine number and dendritic arborization of DLPFC pyramidal neurons relative to those in more posterior regions of the vsWM network.

All four OXPPOS-related mRNAs exhibited decreasing posterior-to-anterior expression gradients across the cortical WM network (Fig. 2E–H). This observation is consistent with a resting state positron emission tomography study [55] showing that the rate of ATP production, calculated from cerebral metabolic rates of oxygen and glucose, was high in V1, intermediate in V2, and low in PPC and DLPFC in healthy human subjects. In general, neurons adjust the expression of OXPPOS-related molecules to meet the changes in ATP demand, supporting their firing and synaptic neurotransmission [17, 18]. For example, in monkey visual cortex, a higher activity of cytochrome oxidase, an enzyme of OXPPOS, was detected in areas with relatively abundant glutamatergic inputs and high neuronal activity [56]. Therefore, the decreasing posterior-to-anterior gradients of OXPPOS-related transcripts could reflect a similar gradient of neuronal activity across the regions. Interestingly, the density of parvalbumin (PV)-positive subsets of GABA neurons is higher in occipital visual regions relative to DLPFC in monkeys [57, 58], which is consistent with a decreasing posterior-to-anterior gradient of PV mRNA levels across cortical regions of the vsWM network in humans [59]. PV neurons are considered to be very energy-demanding due to their high-frequency firing [60] and contain greater numbers of cytochrome oxidase-enriched mitochondria compared with other types of neurons [61]. Therefore, the gradient of OXPPOS-related transcript levels across cortical regions of the WM network could reflect, at least in part, regional differences in PV neuron density. Finally, higher OXPPOS-related transcripts in V1 might reflect the higher ratio of GABA to pyramidal neurons in V1 (1:3) than in other regions (1:4) [62], as GABA neurons have higher cytochrome oxidase activity than pyramidal neurons in monkeys [63, 64].

Alterations of transcripts across cortical regions of the WM network in SZ

The RNAseq and qPCR data showed the same pattern of differences between SZ and UC subjects in the DLPFC. The magnitudes of the disease effect were smaller for all transcripts in the qPCR data (Figs. 1 and 3), but were consistent with the size of the group differences found in prior qPCR studies of these transcripts [14, 16]. The different effect sizes in the RNAseq and qPCR data might reflect differences between studies in assay sensitivity and/or the composition of the subject groups. However, all transcript levels between RNAseq and qPCR measures were positively correlated in the subjects (see Supplementary Table 1) included in both studies (all $r > 0.30$, all $p < 0.04$ with one-tailed t test, $n = 37$).

In SZ, the deficit in the composite actin measure, which is intended to index the activity of actin assembly that promotes the formation and maintenance of spines, was much greater in DLPFC than the other regions (Fig. 4A). This regional difference could be associated with the previously reported greater deficit in spine density of layer 3 pyramidal neurons in DLPFC relative to V1 [10]. This interpretation would appear to not be supported by the significant up-regulation of BAIAP2 in V1 versus DLPFC of SZ subjects. However, in addition to its inhibitory role in spine formation [40, 41], BAIAP2 regulates glutamate transmission as a component of the postsynaptic density [65–67]. In a previous study of the vsWM network of the same subject cohort, transcripts involved in glutamate neurotransmission exhibited the greatest up-regulation in V1 of SZ subjects [47], suggesting that the higher BAIAP2 transcript levels might contribute to altered glutamatergic signaling in V1 of SZ subjects.

In contrast to actin-related transcripts, OXPPOS transcripts were very similar across regions in SZ subjects, suggesting that the magnitude of the disease effect progressively decreased from posterior to anterior regions (Fig. 3E–H). Interestingly, inhibition of OXPPOS enzymes enhanced depolarization-induced glutamate release from isolated synaptosomes [68, 69]. Thus, the prominent down-regulation of OXPPOS transcripts in posterior cortical regions might be associated with the greater alterations in markers of glutamate neurotransmission in these regions in SZ.

The effect of SZ differed between the actin and OXPPOS composite measures across regions of vsWM network, with the disease effect on actin-related transcripts largest in DLPFC and on OXPPOS transcripts largest in V1 (Fig. 4). These opposed regional patterns of disease effect do not seem to support a global cortical disease process of altered actin regulation leading to lower dendritic spine density, reduced pyramidal cell activity and less drive for mitochondrial ATP energy production [26], although the present data are consistent with that idea in the DLPFC (Fig. 4). Furthermore, a comparison of our RNAseq data in the DLPFC to a comparable data set from the anterior cingulate cortex (area 24) of the same subjects [70] revealed that the magnitude of the disease effect on both actin- and OXPPOS-related transcripts differs between these regions (Supplementary Table 2). Thus, the dissociation of actin- and OXPPOS-related composite measures in V1 of SZ subjects suggests that other neuron types, such as PV neurons that exhibited a similar cross-regional pattern in PV mRNA deficits between V1 and DLPFC [59], might contribute to the transcript levels detected in total gray matter in the present study. As PV mRNA levels are regulated by neuronal activity [71], the lower levels of both PV and OXPPOS-related mRNAs in V1 are consistent with lower activity of PV neurons in that region. Although the major excitatory drive to PV neurons is provided by neighboring pyramidal neurons [72], the deficits in actin-related transcripts, which could be associated with lower spine density, were relatively small in V1 compared with DLPFC. Therefore, the prominent deficits in OXPPOS-related transcripts are not likely to be explained solely by lower excitatory drive from pyramidal neurons to PV neurons. Greater deficits in OXPPOS-related transcripts in V1 than DLPFC might not simply reflect a uniform elevation or reduction of the excitatory/inhibitory balance across different cell types and cortical regions in SZ. Indeed, these findings point to the need for cell type-specific assessments of actin- and OXPPOS-related transcripts across regions of the vsWM network in both UC and SZ subjects.

Several lines of evidence suggest that altered transcript levels across cortical regions in SZ are unlikely to be due to other factors commonly associated with the illness. First, in our previous studies, none of the comorbid factors assessed, including substance abuse/dependence at the time of death; use of antidepressants, benzodiazepine/anticonvulsant or antipsychotics at the time of death; or death by suicide had significant effects on actin- or OXPPOS-related transcript levels in the DLPFC of SZ subjects [13, 15, 16, 25, 26, 37, 73]. Second, none of these transcripts exhibited altered expression in the DLPFC of monkeys chronically exposed to antipsychotics at clinically relevant doses [13, 16, 25, 26, 37, 73]. Third, using the current data, none of comorbid factors, such as substance abuse/dependence at the time of death; use of antidepressants, benzodiazepine/anticonvulsants or antipsychotics at the time of death; or death by suicide, had a significant effect on the RNAseq data in DLPFC or on the qPCR data in any cortical region (all $p > 0.1$) (Supplementary Table 4). Fourth, in SZ subjects, none of transcripts showed a significant correlation between the expression levels and the duration of illness in any of the four regions of the WM network (all $|r| < 0.33$, all $p > 0.16$), suggesting that the findings are not a consequence of illness chronicity. Fifth, all individuals with SZ had been living in their communities outside of psychiatric facilities at

the time of death. Finally, we did not detect a significant effect of socio-economic status measured by Hollingshead categorial rankings [74] (Supplementary Tables 1a, b and 4), which might reflect the level of environmental enrichment for each subject, on actin- nor OXPPOS-related transcripts as measured in the DLPFC by RNAseq (all $p > 0.9$) or across the four regions by qPCR (all $p > 0.5$), suggesting that the findings in the individuals with SZ are not due to an impoverished environment.

In conclusion, our analyses of transcript levels across cortical regions in the vsWM network revealed that the transcripts associated with dendritic spine number or energy production had distinct regional expression patterns in UC subjects, suggesting that the strength of local recurrent excitation and energetic demand required for information processing normally differs across cortical regions of the WM network. In SZ, the differential alterations in markers of actin assembly and energy production across regions of the cortical vsWM network suggest that each region may make specific contributions to vsWM impairments in the illness.

REFERENCES

- Kahn RS, Keefe RS. Schizophrenia is a cognitive illness: time for a change in focus. *JAMA Psychiatry*. 2013;70:1107–12.
- Green MF, Horan WP, Lee J. Nonsocial and social cognition in schizophrenia: current evidence and future directions. *World Psychiatry*. 2019;18:146–61.
- Linden DE. The working memory networks of the human brain. *Neuroscientist*. 2007;13:257–67.
- Christophel TB, Klink PC, Spitzer B, Roelfsema PR, Haynes JD. The Distributed Nature of Working Memory. *Trends Cogn Sci*. 2017;21:111–24.
- Goldman-Rakic PS. Cellular basis of working memory. *Neuron*. 1995;14:477–85.
- Constantinidis C, Williams GV, Goldman-Rakic PS. A role for inhibition in shaping the temporal flow of information in prefrontal cortex. *Nat Neurosci*. 2002;5:175–80.
- Courtin J, Chaudun F, Rozeske RR, Karalis N, Gonzalez-Campo C, Wurtz H, et al. Prefrontal parvalbumin interneurons shape neuronal activity to drive fear expression. *Nature*. 2014;505:92–6.
- Glausier JR, Lewis DA. Mapping pathologic circuitry in schizophrenia. *Handb Clin Neurol*. 2018;150:389–417.
- Coyle JT. Glutamate and schizophrenia: beyond the dopamine hypothesis. *Cell Mol Neurobiol*. 2006;26:365–84.
- Glantz LA, Lewis DA. Decreased dendritic spine density on prefrontal cortical pyramidal neurons in schizophrenia. *Arch Gen Psychiatry*. 2000;57:65–73.
- Konopaskie GT, Lange N, Coyle JT, Benes FM. Prefrontal cortical dendritic spine pathology in schizophrenia and bipolar disorder. *JAMA Psychiatry*. 2014;71:1323–31.
- Garey LJ, Ong WY, Patel TS, Kanani M, Davis A, Mortimer AM, et al. Reduced dendritic spine density on cerebral cortical pyramidal neurons in schizophrenia. *J Neurol Neurosurg Psychiatry*. 1998;65:446–53.
- Datta D, Arion D, Corradi JP, Lewis DA. Altered expression of CDC42 signaling pathway components in cortical layer 3 pyramidal cells in schizophrenia. *Biol Psychiatry*. 2015;78:775–85.
- Ide M, Lewis DA. Altered cortical CDC42 signaling pathways in schizophrenia: implications for dendritic spine deficits. *Biol Psychiatry*. 2010;68:25–32.
- Hill JJ, Hashimoto T, Lewis DA. Molecular mechanisms contributing to dendritic spine alterations in the prefrontal cortex of subjects with schizophrenia. *Mol Psychiatry*. 2006;11:557–66.
- Datta D, Arion D, Roman KM, Volk DW, Lewis DA. Altered expression of ARP2/3 complex signaling pathway genes in prefrontal layer 3 pyramidal cells in Schizophrenia. *Am J Psychiatry* 2017;174:163–71.
- Harris JJ, Jolivet R, Attwell D. Synaptic energy use and supply. *Neuron*. 2012;75:762–77.
- Hall CN, Klein-Flugge MC, Howarth C, Attwell D. Oxidative phosphorylation, not glycolysis, powers presynaptic and postsynaptic mechanisms underlying brain information processing. *J Neurosci*. 2012;32:8940–51.
- Magistretti PJ, Allaman I. A cellular perspective on brain energy metabolism and functional imaging. *Neuron*. 2015;86:883–901.
- Maurer I, Zierz S, Moller H. Evidence for a mitochondrial oxidative phosphorylation defect in brains from patients with schizophrenia. *Schizophrenia Res*. 2001;48:125–36.
- Iwamoto K, Bundo M, Kato T. Altered expression of mitochondria-related genes in postmortem brains of patients with bipolar disorder or schizophrenia, as revealed by large-scale DNA microarray analysis. *Hum Mol Genet*. 2005;14:241–53.

22. Park HJ, Lee JD, Chun JW, Seok JH, Yun M, Oh MK, et al. Cortical surface-based analysis of 18F-FDG PET: measured metabolic abnormalities in schizophrenia are affected by cortical structural abnormalities. *NeuroImage*. 2006;31:1434–44.
23. Dreher JC, Koch P, Kohn P, Apud J, Weinberger DR, Berman KF. Common and differential pathophysiological features accompany comparable cognitive impairments in medication-free patients with schizophrenia and in healthy aging subjects. *Biol Psychiatry*. 2012;71:890–7.
24. Hazlett EA, Buchsbaum MS, Jau LA, Nenadic I, Fleischman MB, Shihabuddin L, et al. Hypofrontality in unmedicated schizophrenia patients studied with PET during performance of a serial verbal learning task. *Schizophrenia Res*. 2000;43:33–46.
25. Arion D, Corradi JP, Tang S, Datta D, Boothe F, He A, et al. Distinctive transcriptome alterations of prefrontal pyramidal neurons in schizophrenia and schizoaffective disorder. *Mol Psychiatry*. 2015;20:1397–405.
26. Glausier JR, Enwright JF 3rd, Lewis DA. Diagnosis- and cell type-specific mitochondrial functional pathway signatures in schizophrenia and bipolar disorder. *Am J Psychiatry*. 2020;177:1140–50.
27. Wong-Riley MT. Bigenomic regulation of cytochrome c oxidase in neurons and the tight coupling between neuronal activity and energy metabolism. *Adv Exp Med Biol*. 2012;748:283–304.
28. Liu QA, Shio H. Mitochondrial morphogenesis, dendrite development, and synapse formation in cerebellum require both Bcl-w and the glutamate receptor delta 2. *PLoS Genet*. 2008;4:e1000097.
29. Li Z, Okamoto K, Hayashi Y, Sheng M. The importance of dendritic mitochondria in the morphogenesis and plasticity of spines and synapses. *Cell*. 2004;119:873–87.
30. Amatrudo JM, Weaver CM, Crimins JL, Hof PR, Rosene DL, Luebke JI. Influence of highly distinctive structural properties on the excitability of pyramidal neurons in monkey visual and prefrontal cortices. *J Neurosci*. 2012;32:13644–60.
31. González-Burgos G, Miyamae T, Krimer Y, Gulchina Y, Pafundo DE, Krimer O, et al. Distinct properties of layer 3 pyramidal neurons from prefrontal and parietal areas of the monkey neocortex. *J Neurosci*. 2019;39:7277–90.
32. Elston GN, Rosa MG. The occipitoparietal pathway of the macaque monkey: comparison of pyramidal cell morphology in layer III of functionally related cortical visual areas. *Cereb Cortex*. 1997;7:432–52.
33. Elston GN. Pyramidal cells of the frontal lobe: all the more spinous to think with. *J Neurosci*. 2000;20:RC95–RC95.
34. Dubinsky JM. Heterogeneity of nervous system mitochondria: location, location! *Exp Neurol*. 2009;218:293–307.
35. Mansur A, Rabiner EA, Comley RA, Lewis Y, Middleton LT, Huiban M, et al. Characterization of 3 PET tracers for quantification of mitochondrial and synaptic function in healthy human brain: (18)F-BCPP-EF, (11)C-SA-4503, and (11)C-UCB-J. *J Nucl Med*. 2020;61:96–103.
36. Fromer M, Roussos P, Sieberts SK, Johnson JS, Kavanagh DH, Perumal TM, et al. Gene expression elucidates functional impact of polygenic risk for schizophrenia. *Nat Neurosci*. 2016;19:1442–53.
37. Enwright III JF, Huo Z, Arion D, Corradi JP, Tseng G, Lewis DA. Transcriptome alterations of prefrontal cortical parvalbumin neurons in schizophrenia. *Mol Psychiatry*. 2018;23:1606–13.
38. Gandal MJ, Zhang P, Hadjimihael E, Walker RL, Chen C, Liu S, et al. Transcriptome-wide isoform-level dysregulation in ASD, schizophrenia, and bipolar disorder. *Science*. 2018;362.
39. Luo L. Rho GTPases in neuronal morphogenesis. *Nat Rev Neurosci*. 2000;1:173–80.
40. Kast DJ, Dominguez R. Mechanism of IRSp53 inhibition by 14-3-3. *Nat Commun*. 2019;10:483.
41. Kang J, Park H, Kim E. IRSp53/BAIP2 in dendritic spine development, NMDA receptor regulation, and psychiatric disorders. *Neuropharmacology*. 2016;100:27–39.
42. Yan Z, Kim E, Datta D, Lewis DA, Soderling SH. Synaptic actin dysregulation, a convergent mechanism of mental disorders? *J Neurosci*. 2016;36:11411–17.
43. Bergman O, Ben-Shachar D. Mitochondrial oxidative phosphorylation system (OXPHOS) deficits in schizophrenia: possible interactions with cellular processes. *Can J Psychiatry Rev canadienne de Psychiatr*. 2016;61:457–69.
44. Fernandez-Vizcarra E, Zeviani M. Mitochondrial disorders of the OXPHOS system. *FEBS Lett*. 2021;595:1062–106.
45. van Waveren C, Moraes CT. Transcriptional co-expression and co-regulation of genes coding for components of the oxidative phosphorylation system. *BMC Genomics*. 2008;9:18.
46. Ritchie ME, Phipson B, Wu D, Hu Y, Law CW, Shi W, et al. Limma powers differential expression analyses for RNA-sequencing and microarray studies. *Nucleic Acids Res*. 2015;43:e47.
47. Hoftman GD, Diemel SJ, Bazmi HH, Zhang Y, Chen K, Lewis DA. Altered gradients of glutamate and gamma-aminobutyric acid transcripts in the cortical visuospatial working memory network in Schizophrenia. *Biol Psychiatry*. 2018;83:670–79.
48. Keyzers C, Gazzola V, Wagenmakers EJ. Using Bayes factor hypothesis testing in neuroscience to establish evidence of absence. *Nat Neurosci*. 2020;23:788–99.
49. Good IJ. *Theory of Probability* Harold Jeffreys (Third edition, 447 + ix pp., Oxford Univ. Press, 84s.). *Geophys J Int*. 1962;6:555–58.
50. Rajkowska G, Selemon LD, Goldman-Rakic PS. Neuronal and glial somal size in the prefrontal cortex: a postmortem morphometric study of schizophrenia and Huntington disease. *Arch Gen Psychiatry*. 1998;55:215–24.
51. Ligon LA, Steward O. Role of microtubules and actin filaments in the movement of mitochondria in the axons and dendrites of cultured hippocampal neurons. *J Comp Neurol*. 2000;427:351–61.
52. Gonçalves VF, Cappi C, Hagen CM, Sequeira A, Vawter MP, Derkach A, et al. A comprehensive analysis of nuclear-encoded mitochondrial genes in Schizophrenia. *Biol Psychiatry*. 2018;83:780–89.
53. The Network and Pathway Analysis Subgroup of the Psychiatric Genomics Consortium. Psychiatric genome-wide association study analyses implicate neuronal, immune and histone pathways. *Nat Neurosci*. 2015;18:199–209.
54. Pardiñas AF, Holmans P, Pocklington AJ, Escott-Price V, Ripke S, Carrera N, et al. Common schizophrenia alleles are enriched in mutation-intolerant genes and in regions under strong background selection. *Nat Genet*. 2018;50:381–89.
55. Hyder F, Herman P, Bailey CJ, Möller A, Globinsky R, Fullbright RK, et al. Uniform distributions of glucose oxidation and oxygen extraction in gray matter of normal human brain: No evidence of regional differences of aerobic glycolysis. *J Cereb Blood Flow Metab*. 2016;36:903–16.
56. Wong-Riley MT, Tripathi SC, Trusk TC, Hoppe DA. Effect of retinal impulse blockage on cytochrome oxidase-rich zones in the macaque striate cortex. I. Quantitative electron-microscopic (EM) analysis of neurons. *Vis Neurosci*. 1989;2:483–97.
57. Condé F, Lund JS, Lewis DA. The hierarchical development of monkey visual cortical regions as revealed by the maturation of parvalbumin-immunoreactive neurons. *Brain Res Dev Brain Res*. 1996;96:261–76.
58. Diemel SJ, Ciesielski AJ, Bazmi HH, Profozich EA, Fish KN, Lewis DA. Distinct laminar and cellular patterns of GABA neuron transcript expression in monkey prefrontal and visual cortices. *Cereb Cortex*. 2021;31:2345–63.
59. Tsubomoto M, Kawabata R, Zhu X, Minabe Y, Chen K, Lewis DA, et al. Expression of transcripts selective for GABA neuron subpopulations across the cortical visuospatial working memory network in the healthy state and Schizophrenia. *Cereb Cortex*. 2019;29:3540–50.
60. Tremblay R, Lee S, Rudy B. GABAergic interneurons in the neocortex: from cellular properties to circuits. *Neuron*. 2016;91:260–92.
61. Kann O, Papanicolaou IE, Draguhn A. Highly energized inhibitory interneurons are a central element for information processing in cortical networks. *J Cereb Blood Flow Metab*. 2014;34:1270–82.
62. Hendry SH, Schwark HD, Jones EG, Yan J. Numbers and proportions of GABA-immunoreactive neurons in different areas of monkey cerebral cortex. *J Neurosci*. 1987;7:1503–19.
63. Nie F, Wong-Riley MT. Double labeling of GABA and cytochrome oxidase in the macaque visual cortex: quantitative EM analysis. *J Comp Neurol*. 1995;356:115–31.
64. Wong-Riley MT, Carroll EW. Quantitative light and electron microscopic analysis of cytochrome oxidase-rich zones in V II prestriate cortex of the squirrel monkey. *J Comp Neurol*. 1984;222:18–37.
65. Kim MH, Choi J, Yang J, Chung W, Kim JH, Paik SK, et al. Enhanced NMDA receptor-mediated synaptic transmission, enhanced long-term potentiation, and impaired learning and memory in mice lacking IRSp53. *J Neurosci*. 2009;29:1586–95.
66. Chung W, Choi SY, Lee E, Park H, Kang J, Park H, et al. Social deficits in IRSp53 mutant mice improved by NMDAR and mGluR5 suppression. *Nat Neurosci*. 2015;18:435–43.
67. Choi J, Ko J, Racz B, Burette A, Lee JR, Kim S, et al. Regulation of dendritic spine morphogenesis by insulin receptor substrate 53, a downstream effector of Rac1 and Cdc42 small GTPases. *J Neurosci*. 2005;25:869–79.
68. Kilbride SM, Gluchowska SA, Telford JE, O'Sullivan C, Davey GP. High-level inhibition of mitochondrial complexes III and IV is required to increase glutamate release from the nerve terminal. *Mol Neurodegener*. 2011;6:53.
69. Kilbride SM, Telford JE, Tipton KF, Davey GP. Partial inhibition of complex I activity increases Ca-independent glutamate release rates from depolarized synaptosomes. *J Neurochemistry*. 2008;106:826–34.
70. Enwright JF III, Lewis DA. Similarities in cortical transcriptome alterations between Schizophrenia. *Schizophrenia Bull*. 2021;47:1442–51.
71. Cohen SM, Ma H, Kuchibhotla KV, Watson BO, Buzsáki G, Froemke RC, et al. Excitation-transcription coupling in parvalbumin-positive interneurons employs a novel cam kinase-dependent pathway distinct from excitatory neurons. *Neuron*. 2016;90:292–307.
72. Melchitzky DS, González-Burgos G, Barrionuevo G, Lewis DA. Synaptic targets of the intrinsic axon collaterals of supragranular pyramidal neurons in monkey prefrontal cortex. *J Comp Neurol*. 2001;430:209–21.

73. Arion D, Huo Z, Enwright JF, Corradi JP, Tseng G, Lewis DA. Transcriptome alterations in prefrontal pyramidal cells distinguish Schizophrenia from bipolar and major depressive disorders. *Biol Psychiatry*. 2017;82:594–600.
74. Hollingshead AB Four Factor Index of Social Status (dissertation). Yale University. 1975.

AUTHOR CONTRIBUTIONS

Designing the study (SK, TH, JFE, DAL), acquisition of data (SK, KJB, MT, YY, RK), formulating the research questions (SK, TH, MK, TK, DAL), analyzing the data (SK, JFE, KC), and writing the paper (SK, TH, DAL), critical revision of the paper for important intellectual content (all authors), and obtained funding (SK, TH, DAL).

FUNDING INFORMATION

This work was supported by Japan Society for the Promotion of Science (Grants-in-Aid 17K16394, 20K07949 to SK, and 19H03580 to TH) and by NIH grants (MH043784, MH103204 to DAL). DAL receives investigator-initiated research

support from Merck. The other authors report no financial relationships with commercial interests.

COMPETING INTERESTS

The authors declare no competing interests.

ADDITIONAL INFORMATION

Supplementary information The online version contains supplementary material available at <https://doi.org/10.1038/s41386-022-01274-9>.

Correspondence and requests for materials should be addressed to David A. Lewis.

Reprints and permission information is available at <http://www.nature.com/reprints>

Publisher's note Springer Nature remains neutral with regard to jurisdictional claims in published maps and institutional affiliations.